Sparse production but preferential incorporation of recently produced naïve T cells in the human peripheral pool

Nienke Vrisekoop*†, Ineke den Braber*†, Anne Bregje de Boer*†, An F. C. Ruiter‡, Mariëtte T. Ackermans‡, Saskia N. van der Crabben§, Elise H. R. Schrijver*, Gerrit Spierenburg*, Hans P. Sauerwein§, Mette D. Hazenberg*†, Rob J. de Boer¶, Frank Miedema*†, José A. M. Borghans*†¶, and Kiki Tesselaar*†‖

*Department of Immunology, University Medical Center Utrecht, 3508 AB, Utrecht, The Netherlands; †Department of Clinical Viro-Immunology, Sanquin Research Center, and Landsteiner Laboratory, Academic Medical Center, University of Amsterdam, 1000 GG, Amsterdam, The Netherlands; Departments of ‡Clinical Chemistry and §Endocrinology and Metabolism, Academic Medical Center, University of Amsterdam, 1100 DD, Amsterdam, The Netherlands; and ¶Department of Theoretical Biology, Utrecht University, 3584 CH, Utrecht, The Netherlands

Edited by Philippa Marrack, National Jewish Medical and Research Center, Denver, CO, and approved February 28, 2008 (received for review October 12, 2007)

In mice, recent thymic emigrants (RTEs) make up a large part of the naïve T cell pool and have been suggested to be a distinct short-lived pool. In humans, however, the life span and number of RTEs are unknown. Although ^2H_2O labeling in young mice showed high thymic-dependent daily naïve T cell production, long term up- and down-labeling with ^2H_2O in human adults revealed a low daily production of naïve T cells. Using mathematical modeling, we estimated human naïve CD4 and CD8 T cell half-lives of 4.2 and 6.5 years, respectively, whereas memory CD4 and CD8 T cells had half-lives of 0.4 and 0.7 year. The estimated half-life of recently produced naïve T cells was much longer than these average half-lives. Thus, our data are incompatible with a substantial short-lived RTE population in human adults and suggest that the few naïve T cells that are newly produced are preferentially incorporated in the peripheral pool.

recent thymic emigrants | T cell half-lives | T cell production

The role of the thymus in HIV infection is still poorly understood (1, 2). On the one hand, thymic failure has been suggested to play a crucial role in CD4 T cell loss during HIV infection (3), and rapid thymic rebound has been proposed to be responsible for T cell reconstitution during anti-viral treatment (4). However, it has been argued that thymic output in adults might be too low to have a large impact on CD4 T cell depletion (5). In general, these issues are addressed with estimates of thymic output, naïve and memory T cell production rates, and life spans that are simply extrapolated from observations in mice, monkeys, and lymphopenic or irradiated humans (6–11).

Naïve T cells are generally thought to turnover relatively slowly, but it has been suggested that, in mice, a considerable part of the naïve T cell pool consists of RTEs with relatively rapid turnover (9, 10, 12). In humans, naïve T cell numbers, T cell receptor excision circles (TRECs), and expression of CD31 have been used to measure thymic output (7, 13, 14). Dion *et al.* (4) observed rapid changes in the Sj/Vβ TREC ratio within 3 months after infection with HIV, which suggested the presence of a rapidly turning over RTE pool in human adults containing most of the TRECs in the periphery, similar to young rodents and chickens (15, 16). However, because TRECs are long-lived, none of these approaches is specific for T cells that have recently emigrated from the thymus (1, 2, 5), and, therefore, they fail to quantify thymic output in humans.

Peripheral T cell proliferation might also contribute to the maintenance of the naïve T cell pool in human adults; however, it is unclear which fraction of these cells remains in the naïve T cell pool (17). The contribution of RTEs and peripheral T cell proliferation to the maintenance of the naïve T cell pool can only be determined by studying the fate of newly produced T cells. *In vivo* labeling with stable isotopes in combination with appropriate mathematical analysis of these data provides a way to obtain T cell decay and production rates and to follow the fate of recently produced T cells. Data on stable isotope labeling of naïve and memory human T cells (18–22) are available, but several short-comings of these studies hamper their interpretation: (*i*) the short-term labeling period, which did not allow for sufficiently high labeling levels of naïve cells (19, 21, 22); and (*ii*) the lack of delabeling curves in long-term labeling studies (20), which would have shown whether recently produced T cells contribute to the T cell pool under investigation or rapidly disappear by death or activation; and (*iii*) the frequent use of the precursor-product relationship (20, 23, 24), leading to underestimation of the extent of T cell turnover (25). Using the precursor-product relationship one measures the *net* accrual of label and ignores the possibility that cells were produced and lost during the labeling period because of a short life span.

Here, we combined long term *in vivo* stable-isotope labeling and label-decay studies of T cells to obtain sufficient levels of labeling and sufficient data points to allow for reliable parameter fitting, using a mathematical model to estimate naïve T cell production and loss rates. Our analyses showed a slow accumulation of label within the naïve T cell pool, due to low daily production of naïve T cells with a very long half-life. These data are incompatible with the presence of a substantial short-lived RTE pool in human adults.

Results

Thymic Output in Mice. Because the main focus of this study was to establish the role of thymic output and peripheral T cell proliferation in the maintenance of the naïve T cell pool, we first studied whether thymic output—and more specifically, a rapidly turning over RTE pool—could be detected by using the ^2H_2O-labeling technique. It is generally accepted that young rodents have considerable thymic output (26, 27). BrdU-labeling, TREC dynamics and thymic engraftment in mice have revealed that the RTE pool of mice has a fast turnover (10, 15), with an average

Author contributions: N.V., and I.d.B. contributed equally to this work; N.V., I.d.B., H.P.S., R.J.d.B., F.M., J.A.M.B., and K.T. designed research; N.V., I.d.B., A.B.d.B., A.F.C.R., M.T.A., S.N.v.d.C., E.H.R.S., G.S., and M.D.H. performed research; N.V., I.d.B., M.T.A., R.J.d.B., and J.A.M.B. analyzed data; and N.V., I.d.B., R.J.d.B., F.M., J.A.M.B., and K.T. wrote the paper.

The authors declare no conflict of interest.

This article is a PNAS Direct Submission.

‖To whom correspondence should be addressed at: Department of Immunology, University Medical Center Utrecht, Lundlaan 6, P.O. Box 85090, 3508 AB, Utrecht, The Netherlands. E-mail: k.tesselaar@umcutrecht.nl.

This article contains supporting information online at www.pnas.org/cgi/content/full/0709713105/DCSupplemental.

IMMUNOLOGY

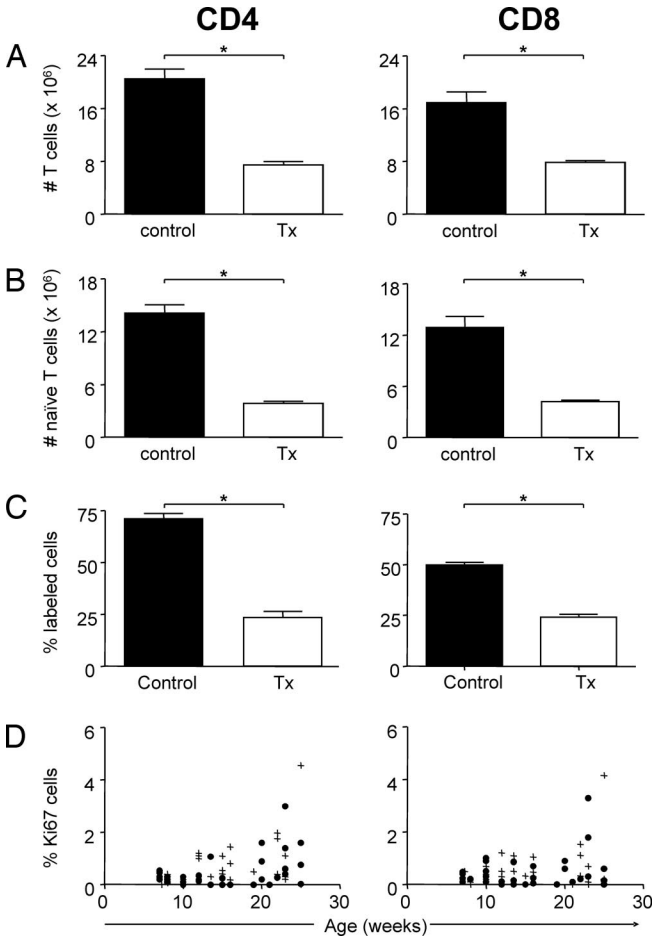

Fig. 1. Thymic output is important for the maintenance of the naïve T cell pool in young mice and can be quantitated by using ^2H_2O labeling. (*A* and *B*) Absolute numbers of total (*A*) and naïve (*B*) CD4 and CD8 T cells in spleen of three control (black bars) and four thymectomized (open bars) animals 14–16 weeks after time of surgery. (*C*) Accumulated ^2H_2O-labeling in naïve CD4 and CD8 T cells of the same euthymic and athymic mice after a 9- to 10-week labeling period. Data are displayed as mean ± standard error of the mean (n = 3–4). *, $P \leq 0.05$ is considered significant. (*D*) Percentage of Ki67$^+$ cells within the naïve CD4 and naïve CD8 T cell pool of control (●) and thymectomized (+) mice at different time points before and after thymectomy.

life span of only 3 weeks (9, 12). We first investigated whether this rapidly turning over RTE pool can be detected in young male mice, using the ^2H_2O-labeling technique, and compared euthymic and thymectomized mice to establish to what extent RTEs affect the labeling within the naïve T cell pool.

Thymectomy of 7-week-old mice resulted in a severe and significant reduction in absolute CD4 and CD8 T cell counts in lymph nodes (LNs) and spleen compared with both age-matched controls (Fig. 1*A*) and sham-thymectomized mice (data not shown). Taking into account the natural reduction in T cell numbers in peripheral lymphoid organs during aging, the fastest decrease in T cell counts was seen in the first 3 weeks after thymectomy. Between 3 and 8 weeks after thymectomy, the number of naïve CD4 and CD8 T cells continued to decline more rapidly than in euthymic mice, whereas at later time points they decreased at approximately similar rates in thymectomized and euthymic mice. Fourteen to 16 weeks after surgery naïve CD4 T cells were reduced by 73% ($P = 0.029$) in spleen and 77% ($P = 0.029$) in LNs, whereas naïve CD8 T cells were reduced by 67% ($P = 0.029$) in spleen and 70% ($P = 0.029$) in LNs (Fig. 1*B* and data not shown).

^2H_2O labeling of young (12- to 13-week-old) euthymic mice for 9–10 weeks resulted in 71 ± 3% up-labeling for naïve CD4 T cells and 50 ± 1% for naïve CD8 T cells in the spleen (Fig. 1*C*). Comparable fractions of labeled cells were found in the LNs (data not shown). This high degree of labeling in T cells could be due to substantial peripheral proliferation of naïve T cells and/or reflect output of labeled thymocytes. To discriminate between these possibilities, mice were thymectomized at the age of 7 weeks and submitted to the long-term ^2H_2O-labeling protocol 5 to 6 weeks later. In the absence of thymic output the fraction of labeled naïve T cells after 10 weeks up-labeling was 2–3-fold reduced (23 ± 3% for naïve CD4 T cells; 24 ± 1% for naïve CD8 T cells, $P = 0.05$) (Fig. 1*C*). Interestingly, the fraction of cycling (Ki67$^+$) naïve T cells was not altered in athymic mice (Fig. 1*D*). This indicates that the difference in labeled naïve T cells between euthymic and thymectomized mice reflects the amount of label that was acquired while dividing in the thymus. Collectively, these data demonstrate that thymic output can be measured by using ^2H_2O labeling. Furthermore, the observation that thymectomy led to a significantly reduced fraction of labeled cells and a significant loss of naïve T cells confirms that, in young mice, RTEs contribute substantially to the naïve T cell pool.

^2H_2O Labeling in Human Volunteers. Next we aimed to determine the role of thymic output and peripheral T cell proliferation in the maintenance of the naïve T cell pool and the turnover rate of the memory T cell pool in five adult humans between 20 and 25 years of age. During the 9-week up-labeling period and subsequent 16-week down-labeling period, blood samples were drawn at 14 time points. Absolute numbers of CD4 and CD8 T cells and the fraction of naïve CD45RO$^-$CD27$^+$ and memory CD45RO$^+$ CD4 and CD8 T cells were measured, and these fractions were sorted for measurement of deuterium enrichment in the DNA. In addition, we measured *ex vivo* proliferation by the expression of the proliferation marker Ki67 within these same naïve and memory T cell populations to exclude the possibility that episodes of overt immune activation affected turnover rates. Characteristics of the healthy volunteers are given in supporting information (SI) Table S1.

Body Water and Granulocyte Enrichment. As a measure for body water enrichment during up- and down-labeling, we quantified ^2H_2O enrichment in urine at each time point. At the earliest time points after start of ^2H_2O labeling, body water enrichment had not yet reached its maximum level, whereas shortly after cessation of label body water was still found to be enriched. Therefore, we modeled the body water enrichment curves (see *SI Text* and Fig. S1) and corrected for these best fits when analyzing the enrichment in the different cell populations. Because granulocytes are known to turnover rapidly, labeling of the granulocyte population of each individual was measured to estimate the maximal level of label intake that cells could possibly attain (see *SI Text* and Fig. S1). Furthermore, because DNA baseline enrichment is not only determined by naturally occurring extremely low ^2H_2O enrichment, but also by the more abundant naturally occurring heavy carbon atoms, we also longitudinally measured a negative control who did not drink ^2H_2O, which pointed out that background fluctuations were negligible (data not shown).

Turnover of Naïve and Memory CD4 and CD8 T Cells. First of all, all labeling data of the different T cell subsets were divided by the estimated maximum granulocyte enrichment of each volunteer (see *SI Text*). The mathematical model was used to fit the corrected data, and to determine the average turnover rate (p) and the average rate at which labeled cells were lost from the population (d). It is important to realize that the accrual of label during label administration is truly representative of the T cell population as a whole, whereas the loss of label after label cessation is only based on those cells that have picked up label by cell division. Therefore, we based our analyses on a so-called kinetic heterogeneity model in which the

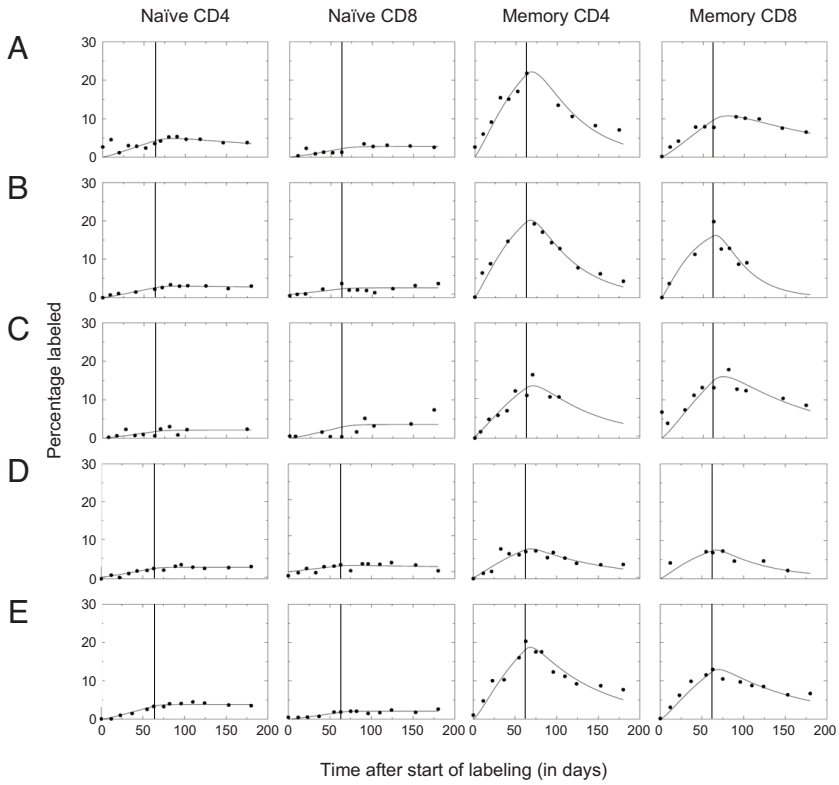

Fig. 2. Best fits of the naïve and memory CD4 and CD8 T cell enrichment curves. Label enrichment was scaled between 0 and 100% by normalizing for the percentage label obtained in granulocytes (see *SI Text*). In the graph, the end of the labeling period is marked by a vertical line.

average turnover rate of the T cell population is not necessarily equal to the loss rate of labeled cells (28).

The median turnover rates of naïve CD4 and CD8 T cells were found to be as low as $p = 0.0005$ and 0.0003 per day, corresponding to median half-lives of 1,517 and 2,374 days for naïve CD4 and CD8 T cells, respectively (Fig. 2 and Tables 1 and 2). The turnover rates of memory CD4 and CD8 T cells were found to be ≈10-fold higher, i.e., $p = 0.0045$ and 0.0028 per day, corresponding to half-lives of 155 and 244 days for memory CD4 and CD8 T cells, respectively. Using the individual naïve CD4 and CD8 T cell counts revealed a median naïve CD4 T cell production of 8.2×10^7 cells per day and a median naïve CD8 T cell production of 2.4×10^7 per day (Table 3). Because this daily production of new naïve T cells is the sum of thymic output and homeostatic proliferation within the naïve T cell pool, our data provide an upper estimate of daily thymic production of 1.7×10^8 T cells per day (see Table 3).

The median rates at which labeled memory CD4 and CD8 T cells were lost from the memory population were found to be 0.0145 and 0.0098 per day, respectively. Interestingly, in none of the individuals did we find a significant loss of labeled naïve CD4 or CD8 T cells during the 16 weeks after cessation of label (Fig. 2 and Table 1), indicating that newly produced naïve T cells—whether produced by the thymus or by peripheral T cell proliferation—had a longer expected life span than the average naïve T cell. Our data are therefore not compatible with the presence of a substantial short-lived RTE pool in adult healthy humans.

Discussion

By *in vivo* labeling of T cell subsets using ^2H_2O and mathematical analysis of label enrichment, our data provide reliable estimates for the average turnover rates of naïve and memory CD4 and CD8 T cells in healthy adults. Although isotope labeling studies in humans are typically restricted to blood, it has been reported that labeling kinetics in human T cells derived from blood and lymphoid tissues are comparable (29). Label incorporation in T cells derived from mouse peripheral lymph nodes and spleen was also similar (unpublished data). Seemingly, there is little difference in labeling of the analyzed T cell subsets derived from the different lymphoid compartments.

The very low accumulation of label in naïve T cells (<5%) that we observed after 9 weeks of up-labeling is compatible with the data reported by Hellerstein *et al.* (20). Our median estimated half-lives between 1,517 and 2,374 days for naïve T cells and between 155 and 244 days for memory T cells are, however, much longer than previous estimates based on stable-isotope labeling, which varied from 112 to 361 days for naïve T cells and from 14 to 235 days for memory T cells (25). The use of T cell death rates, which overestimate T cell turnover because of the bias toward cells that have recently divided (30), and the lack of data points during the up-labeling phase in previous short-term labeling experiments might explain these discrepancies. Michie *et al.* (6) used the presence of T cells with dicentric chromosomes after radiation to measure the half-life of naïve and memory T cells. They estimated a half-life of 182 days for $CD45RO^+$ and 630 days for $CD45RA^+$ T cells. Because $CD45RA^+$ T cells can contain a substantial fraction of effector ($CD45RA^+CD27^-$) cells, we additionally used CD27 expression on $CD45RA^+$ T cells to identify naïve T cells. This difference in definition of the naïve subset may explain the difference in the estimated life spans between these studies. Furthermore, it is conceivable that the half-lives of T cells were affected by radiation.

The origin of variation in the calculated half-lives of the adult humans is unknown: No relation was found between this parameter and T cell counts, Ki67 expression, or age. The relative differences in calculated half-lives were, however, in the same range as the

Table 1. Turnover rates (p) and loss rates of labeled cells (d) per day

Cell	Variable	Individual A	B	C	D	E	Median
Naïve $CD4^+$	p	0.0009 (0.0007–0.0015)	0.0005 (0.0004–0.0005)	0.0003 (0.0002–0.0005)	0.0004 (0.0003–0.0004)	0.0006 (0.0005–0.0006)	0.0005
	d	0.0040 (0.0000–0.0106)	0.0009 (0.0000–0.0029)	0.0000 (0.0000–0.0083)	0.0000 (0.0000–0.0026)	0.0000 (0.0000–0.0010)	0.0000
Naïve $CD8^+$	p	0.0004 (0.0003–0.0006)	0.0003 (0.0002–0.0003)	0.0005 (0.0003–0.0010)	0.0003 (0.0001–0.0005)	0.0003 (0.0002–0.0004)	0.0003
	d	0.0000 (0.0000–0.0050)	0.0000 (0.0000–0.0000)	0.0000 (0.0000–0.0119)	0.0024 (0.0000–0.0132)	0.0000 (0.0000–0.0000)	0.0000
Memory $CD4^+$	p	0.0067 (0.0059–0.0081)	0.0058 (0.0052–0.0068)	0.0034 (0.0026–0.0044)	0.0017 (0.0014–0.0022)	0.0045 (0.0040–0.0052)	0.0045
	d	0.0203 (0.0158–0.0250)	0.0198 (0.0163–0.0227)	0.0145 (0.0069–0.0230)	0.0115 (0.0070–0.0161)	0.0126 (0.0094–0.0154)	0.0145
Memory $CD8^+$	p	0.0021 (0.0018–0.0025)	0.0060 (0.0043–0.0083)	0.0034 (0.0029–0.0046)	0.0019 (0.0014–0.0028)	0.0028 (0.0025–0.0034)	0.0028
	d	0.0065 (0.0041–0.0096)	0.0304 (0.0192–0.0436)	0.0089 (0.0040–0.0133)	0.0161 (0.0077–0.0262)	0.0098 (0.0071–0.0127)	0.0098

Depicted are turnover rates (p) and loss rates of labeled cells (d) per day as estimated by the mathematical model. The 95% confidence intervals (in parentheses) were determined by bootstrapping (44), resampling the residuals 500 times.

Table 2. Half-lives of naïve and memory $CD4^+$ and $CD8^+$ T cells

Cell	Individual A	B	C	D	E	Median
Naïve $CD4^+$	801	1,517	2,374	1,899	1,187	1,517
Naïve $CD8^+$	1,737	2,762	1,341	2,398	2,374	2,374
Memory $CD4^+$	104	119	204	402	155	155
Memory $CD8^+$	327	116	202	359	244	244

Depicted are half-lives ($\ln 2/p$) in days derived from the mathematical model.

differences in the other parameters that we and others have measured (31).

The maximum total daily naïve T cell production in our five healthy volunteers of 13.1×10^7 CD4 T cells and 3.5×10^7 CD8 T cells implies that the thymus in human adults is exporting maximally 1.7×10^8 T cells per day. Part of the labeling of the naïve T cell population may, however, also be due to peripheral T cell proliferation. The estimated total daily naïve T cell production is in close agreement with the daily accumulation of 10^8 naïve T cells in patients with a depleted T cell pool (8, 32), which suggests that thymic output and naïve T cell proliferation do not homeostatically respond to that level of peripheral T cell depletion. Still, the production of naïve T cells in such depleted situations might be underestimated because naïve T cells may transit more rapidly to the memory pool.

Our analyses also enabled us to follow the fate of recently produced cells. In the memory T cell population, we found that the decay rate of labeled cells is higher than the average production rate, indicating that the turnover of cells that picked up label was higher than the turnover of the average cell in the memory population. This finding is in line with previous labeling studies, which all showed that the loss of labeled cells exceeded their production (28, 30, 33). Unexpectedly, we found that this was not the case for the naïve T cell population, because no significant loss of labeled cells was observed in any of the five individuals during the 16 weeks after label cessation. Thus, newly produced (i.e., labeled) naïve T cells, whether produced by the thymus or by peripheral proliferation, tended to live longer than the average cell in the naïve T cell population. This implies that newly produced naïve T cells were preferentially incorporated into the peripheral naïve T cell pool, which contradicts the notion of a substantial short-lived RTE pool in human adults.

To be sure that administration of ^2H_2O would efficiently label thymic emigrants, we performed ^2H_2O labeling in euthymic and thymectomized mice. Studies have shown that thymic output in young rodents is substantial (26, 27), and TREC dynamics, BrdU labeling, and thymic engraftment have demonstrated that the RTE pool in mice has a fast turnover (9, 10, 12, 15). In line with previous studies, we found that thymectomy in young mice gives a considerable reduction in peripheral naïve T cell numbers already within 3 weeks after thymectomy (34, 35), indicating an important contribution of RTEs to the naïve T cell population in young mice.

Table 3. Total production of naïve T cells per day

Cell	Individual A	B	C	D	E	Median
$CD4^+$	11.50	5.36	2.24	8.19	13.10	8.19
$CD8^+$	2.53	1.51	2.39	2.07	3.53	2.39
Total	14.03	6.87	4.63	10.26	16.63	10.26

Total production of naïve T cells per day ($\times 10^7$), calculated as $p \times$ [the naïve T cell count per liter blood] $\times$ [5 liter blood] $\times$ 50, assuming that 2% of lymphocytes reside in the blood (45).

Thymectomy induced a 2- to 3-fold decrease in labeled naïve T cells, showing that the ^2H_2O protocol successfully labeled RTEs in euthymic mice.

In thymectomized mice, T cell numbers were severely reduced. It has been described that, under lymphopenic circumstances, homeostatic naïve T cell proliferation and conversion to a memory phenotype occurs (36). Whether reversion of memory T cells to a naïve phenotype occurs, is still unclear (37). Because no increase in the fraction of $Ki67^+$ naïve or effector/memory T cells was observed in thymectomized mice, the residual labeling of naïve T cells is most likely not due to homeostatic proliferation or reversion. For the human study, we can formally not rule out the possibility of conversion; but, because we performed the study in healthy persons with normal T cell counts, one may expect very low conversion and reversion rates.

Our data shed a different light on thymic output and RTE dynamics. In contrast to the observations by Berzins *et al.*, which suggested that, in young mice, an excess of short-lived RTEs is produced that is displaced 3 weeks after export from the thymus (12), we found that, in human adults, RTEs are rare and long-lived and thus remain in the peripheral T cell pool. The advantage of a short-lived RTE pool has been proposed to be the continuous supply of T cells with a diverse repertoire to the long-lived resident naïve T cell pool (38). The preferential incorporation of RTEs into the resident naïve T cell pool that we here describe for human adults seems a much more efficient way to continuously rejuvenate the naïve T cell pool and repertoire than a daily excess production of RTEs with a very short life span. However, the unfortunate consequence of this sparse production of long-lived naïve T cells is that naïve T cell supply may be limiting in clinical conditions of chronic T cell depletion, and—because of the increasing life expectancy—even in healthy elderly, which may have severe clinical consequences.

Taken together, our data confirm the presence of a significant RTE pool with rapid turnover in young mice, whereas in human adults recently produced naïve T cells are rare and long-lived.

Materials and Methods

Mouse Studies. ***Mice.*** C57BL/6 mice were maintained by in-house breeding at the Netherlands Cancer Institute (Amsterdam) under specific pathogen-free conditions in accordance with institutional and national guidelines. To exclude possible gender effects, we only used male mice in this study.

Thymectomy. Seven-week-old male C57BL/6 mice were anesthesized by i.p. injection with Hypnorm (0.4 mg/kg fentanyl citrate and 12.5 mg/kg fluanisone; Janssen Animal Health) and Dormicum (6.3 mg/kg; Roche). The mouse was placed in supine position, and its limbs and maxilla were taped to a surgical board. The skin was prepped with 70% alcohol. A midline incision was made from the lower cervical region to the level of the fifth rib. The skin was loosened, and the salivary glands were pushed laterally. Directly adjacent to the sternum the two upper ribs were cut, thereby exposing the thymus. Vacuum suction was applied to remove the organ. The skin was closed by interrupted sutures, and the animals were warmed until recovery from anesthesia. Postoperative survival was 85%. The completeness of thymectomy was confirmed by visual inspection both directly after removal of the organ and at the conclusion of the experiment.

^2H_2O labeling protocol. Twelve- to 13-week-old animals obtained one boost injection (i.p.) of 15 ml/kg with 99.8% ^2H_2O (Cambridge Isotopes) and were subsequently fed with 4% ^2H_2O for 9 or 10 weeks (control and thymectomized mice, respectively).

FACS staining and cell sorting. Because of the limited amount of blood that can be drawn from mice and the amount of cells needed for GC/MS analysis, we were unable to isolate enough cells of each T cell subset from blood derived from (thymectomized) mice. Therefore, thymus, spleen and (axillary, brachial, inguinal, and superficial cervical) LNs were isolated from 21- to 23-week-old thymectomized and control C57BL/6 mice. Single-cell suspensions were obtained by mechanical disruption. Red blood cells were lysed with ammonium chloride solution [155 mM NH_4Cl, 10 mM $KHCO_3$, and 0.1 mM EDTA (pH 7.4)]. Cells were washed, resuspended in IMDM/7% FCS, and counted. Cells (5×10^5 per well) were seeded in 96-well plates in FACS staining buffer (PBS/1% FCS) and stained with CD4-PerCP or CD8-PerCP, CD44-APC, and CD62L-PE (BD PharMingen) in the presence of blocking 2.4G2 mAb (CD16/CD32). After incubation with Cytofix/cytoperm solution (BD PharMingen), the cells were incubated with Ki67-FITC or IgG-FITC (BD) in 0.1% saponin (in FACS staining buffer). Cells were analyzed on a LSR II flow cytometer and with BD PharMingen FACSDiva software. For logistical reasons, splenocytes were left overnight at room temperature, and stained the next day for CD4-PerCP, CD8-FITC, CD44-APC, and CD62L-PE (BD PharMingen). Cell recovery after overnight storage was usually 77%. Preferential loss of particular T cell subsets was not observed. Naïve ($CD62L^+$, $CD44^-$) cells were sorted by using a FACSAria cell sorter and FACSDiva software (BD PharMingen). Purity of the sorted cells was 81–97% for naïve CD4 T cells (average: 96% for control vs. 83% for thymectomized mice) and 86–99% for naïve CD8 T cells (average: 98% for control vs. 88% for thymectomized mice). Granulocytes were isolated by density gradient centrifugation of blood, using a combination of histopaque-1119 and Ficoll-paque followed by red blood cell lysis. Granulocytes and thymocytes were frozen until further processed.

Statistical analysis. The Mann–Whitney test was performed to determine differences between mouse groups. All statistical analyses were performed by using the software program SPSS 12.0. Differences with $P \leq 0.05$ were considered significant.

Human Studies. ***Subjects and in vivo ^2H_2O labeling protocol.*** Five healthy male volunteers (characteristics of the T cell compartment of these volunteers are given in Table S1) were submitted to the AMC hospital to receive the initial administration dose of 10 ml of ^2H_2O per kilogram of body water in small portions throughout the day. Body water was estimated to be 60% of body weight. As a maintenance dose, the subjects daily drank 1/8 of this initial dose at home for 9 weeks. Blood and urine were collected before labeling, after the boost of label at the end of day 0, and six times during the labeling protocol. In addition, during the down-label phase of 16 weeks blood and urine were collected seven times. All patients were healthy and were asked to answer a questionnaire to exclude (a high risk of) infections and immunomodulatory medication. This study was approved by the medical ethical committee of the Academic Medical Center, and written informed consent was obtained from all volunteers.

Flow cytometry and cell sorting. Absolute CD4 and CD8 T cell counts were determined by dual-platform flow cytometry.

Peripheral blood mononuclear cells (PBMC) were obtained by Ficoll-Paque density gradient centrifugation from heparinized blood and cryopreserved until further processed. Peripheral blood T cell proliferation in CD4 and CD8 T cell subsets was studied by flow-cytometric measurements of Ki67 nuclear antigen, as described in refs. 39–41.

To measure the fraction of labeled cells within the naïve ($CD45RO^-CD27^+$) and memory ($CD45RO^+$) CD4 and CD8 T cell population, cryopreserved PBMC were thawed and incubated with monoclonal antibodies (mAb) to CD45RO-FITC (Caltag), CD27-PE, CD4-PerCP, and CD8-APC (BD PharMingen). The specified cell fractions were isolated by cell sorting on a MoFlow high speed cell sorter or on a FACSAria (BD PharMingen). Purity of the sorted cells was, on average, 96% for naïve CD4 and CD8 T cells, 95% for memory $CD4^+$ T cells, and 91% for memory CD8 T cells.

Measurement of ^2H_2O enrichment in body water and DNA. Deuterium enrichment in urine was measured by a method adopted from Previs *et al.* (42). The isotopic enrichment of DNA was measured according to the method described by Neese *et al.* (18) with minor modifications. Briefly, DNA was enzymatically hydrolyzed into deoxyribonucleotides, after which the deoxyadenosines were purified by using a SPE column. The adenosine residue was captured by cation resin, and the deoxyribose was derivatized to deoxyribosepentane-tetraacetate (PTA) before injection into the gas chromatograph (6890 series; Agilent Technologies). The mass of the derivate was measured by positive chemical ionization mass spectrometry (5973 MSD; Agilent Technologies) at m/z 245 (M_0) and 246 (M_1). Because M_1 is known to be concentration-dependent, we first used the peak area at M_0 to determine the suspected natural abundance for each sample (43). The enrichment (EM_1) was subsequently determined by dividing the peak area at M_1 by the total peak area ($M_1 + M_0$) after subtraction of the corrected natural abundance from the measured M_1 enrichment. We first fitted the urine enrichment data of each individual to a simple label enrichment/decay curve (see Fig. S1 and Table S2). The best fits for urine enrichment were incorporated when analyzing the enrichment in the different cell populations. Up- and down-labeling of the granulocyte population of each individual was analyzed mathematically to determine the maximal level of label intake that cells could possibly attain (see Fig. S1 and Table S3). The average turnover rate and the loss rate of labeled cells in each T cell subset were determined after normalization by this granulocyte maximum (see *SI Text*). For ease of the procedure, mouse thymocytes were used (if available) to determine the maximal level of label intake. In thymectomized mice the enrichment of fully turned-over granulocytes was used as indicator, because maximal label enrichment in mouse thymocytes and granulocytes was found to be similar.

Supporting Information. The mathematical model is described in *SI Text*. The characteristics of the T cell compartment of the human volunteers are described in Table S1. Fig. S1 shows the best fit for urine and relative granulocyte

enrichment. Tables S2 and S3 give the estimated parameters for urine and granulocytes, respectively. Deuterium enrichment in urine and in the DNA of granulocytes and T cell subsets (EM_1) of all individuals is given in Dataset S1.

ACKNOWLEDGMENTS. We thank Marc Hellerstein and Rich Neese for sharing the ^2H_2O labeling and GC/MS protocols, Loes Rijswijk for improving the thymectomy procedure in mice, and Alan Perelson and Becca Asquith for very useful suggestions and discussions. This research was supported by AIDS Fonds Netherlands Grants 4025, 4024, and 7010; Netherlands Organization for Scientific Research Grants 916.36.003 and 016.048.603; Human Frontier Science Program Grant RGP0010/2004; and Landsteiner Foundation for Blood Research Grant 0210.

1. Hazenberg MD, Borghans JAM, De Boer RJ, Miedema F (2003) Thymic output: A bad TREC record. *Nat Immunol* 4:97–99.
2. Douek D (2004) Thymic output and HIV infection: On the right TREC. *Immunity* 21:744–745.
3. Douek DC, *et al.* (2001) Evidence for increased T cell turnover and decreased thymic output in HIV infection. *J Immunol* 167:6663–6668.
4. Dion ML, *et al.* (2004) HIV infection rapidly induces and maintains a substantial suppression of thymocyte proliferation. *Immunity* 21:757–768.
5. Hazenberg MD, *et al.* (2000) Increased cell division but not thymic dysfunction rapidly affects the TREC content of the naive T cell population in HIV-1 infection. *Nature Med* 6:1036–1042.
6. Michie CA, McLean A, Alcock C, Beverley PCL (1992) Lifespan of human lymphocyte subsets defined by CD45 isoforms. *Nature* 360:264–265.
7. Mackall CL, *et al.* (1995) Age, thymopoiesis, and $CD4^+$ T-lymphocyte regeneration after intensive chemotherapy. *N Engl J Med* 332:143–149.
8. Clark DR, De Boer RJ, Wolthers KC, Miedema F (1999) T cell dynamics in HIV-1 infection. *Adv Immunol* 73:301–327.
9. Berzins SP, Godfrey DI, Miller JF, Boyd RL (1999) A central role for thymic emigrants in peripheral T cell homeostasis. *Proc Natl Acad Sci USA* 96:9787–9791.
10. Tough DF, Sprent J (1994) Turnover of naive- and memory-phenotype T cells. *J Exp Med* 179:1127–1135.
11. Arron ST, *et al.* (2005) Impact of thymectomy on the peripheral T cell pool in rhesus macaques before and after infection with simian immunodeficiency virus. *Eur J Immunol* 35:46–55.
12. Berzins SP, Boyd RL, Miller JFAP (1998) The role of the thymus and recent thymic migrants in the maintenance of the adult peripheral lymphocyte pool. *J Exp Med* 187:1839–1848.
13. Douek DC, *et al.* (1998) Changes in thymic function with age and during the treatment of HIV infection. *Nature* 396:690–695.
14. Kimmig S, *et al.* (2002) Two subsets of naive T helper cells with distinct T cell receptor excision circle content in human adult peripheral blood. *J Exp Med* 195:789–794.
15. Sempowski GD, *et al.* (2002) T cell receptor excision circle assessment of thymopoiesis in aging mice. *Mol Immunol* 38:841–848.
16. Kong FK, *et al.* (1999) T cell receptor gene deletion circles identify recent thymic emigrants in the peripheral T cell pool. *Proc Natl Acad Sci USA* 96:1536–1540.
17. Grossman Z, *et al.* (2002) CD4 T cell depletion in HIV infection: Are we closer to understanding the cause? *Nat Med* 8:319–323.
18. Neese RA, *et al.* (2002) Measurement *in vivo* of proliferation rates of slow turnover cells by ^2H_2O labeling of the deoxyribose moiety of DNA. *Proc Natl Acad Sci USA* 99:15345–15350.
19. Macallan DC, *et al.* (2003) Measurement and modeling of human T cell kinetics. *Eur J Immunol* 33:2316–2326.
20. Hellerstein MK, *et al.* (2003) Subpopulations of long-lived and short-lived T cells in advanced HIV-1 infection. *J Clin Invest* 112:956–966.
21. Macallan DC, *et al.* (2004) Rapid turnover of effector-memory $CD4^+$ T cells in healthy humans. *J Exp Med* 200:255–260.
22. Wallace DL, *et al.* (2004) Direct measurement of T cell subset kinetics *in vivo* in elderly men and women. *J Immunol* 173:1787–1794.
23. Hellerstein MK, Neese RA (1992) Mass isotopomer distribution analysis: A technique for measuring biosynthesis and turnover of polymers. *Am J Physiol* 263:E988–E1001.
24. Macallan DC, *et al.* (1998) Measurement of cell proliferation by labeling of DNA with stable isotope-labeled glucose: Studies *in vitro*, in animals, and in humans. *Proc Natl Acad Sci USA* 95:708–713.
25. Borghans JAM, De Boer RJ (2007) Quantification of T cell dynamics: From telomeres to DNA labelling. *Immunol Rev* 216:35–47.
26. Weissman IL (1967) Thymus cell migration. *J Exp Med* 126:291–304.
27. Scollay RG, Butcher EC, Weissman IL (1980) Thymus cell migration. Quantitative aspects of cellular traffic from the thymus to the periphery in mice. *Eur J Immunol* 10:210–218.
28. Asquith B, *et al.* (2002) Lymphocyte kinetics: The interpretation of labelling data. *Trends Immunol* 23:596–601.
29. Kovacs JA, *et al.* (2005) Induction of prolonged survival of $CD4^+$ T lymphocytes by intermittent IL-2 therapy in HIV-infected patients. *J Clin Invest* 115:2139–2148.
30. Grossman Z, Herberman RB, Dimitrov DS (1999) T cell turnover in SIV infection. *Science* 284:555a.
31. Comans-Bitter WM, *et al.* (1997) Immunophenotyping of blood lymphocytes in childhood. Reference values for lymphocyte subpopulations. *J Pediatr* 130:388–393.
32. Cohen SJ, *et al.* (2002) Reconstitution of naive T cells during antiretroviral treatment of HIV-infected adults is dependent on age. *AIDS* 16:2263–2266.
33. Ribeiro RM, Mohri H, Ho DD, Perelson AS (2002) *In vivo* dynamics of T cell activation, proliferation, and death in HIV-1 infection: Why are $CD4^+$ but not $CD8^+$ T cells depleted? *Proc Natl Acad Sci USA* 99:15572–15577.
34. Budd RC, *et al.* (1987) Distinction of virgin and memory T lymphocytes. Stable acquisition of the Pgp-1 glycoprotein concomitant with antigenic stimulation. *J Immunol* 138:3120–3129.
35. Di Rosa F, Ramaswamy S, Ridge JP, Matzinger P (1999) On the lifespan of virgin T lymphocytes. *J Immunol* 163:1253–1257.
36. Tanchot C, *et al.* (2002) Conversion of naive T cells to a memory-like phenotype in lymphopenic hosts is not related to a homeostatic mechanism that fills the peripheral naive T cell pool. *J Immunol* 168:5042–5046.
37. Ge Q, Hu H, Eisen HN, Chen J (2002) Different contributions of thymopoiesis and homeostasis-driven proliferation to the reconstitution of naive and memory T cell compartments. *Proc Natl Acad Sci USA* 99:2989–2994.
38. Berzins SP, *et al.* (2002) Thymic regeneration: Teaching an old immune system new tricks. *Trends Mol Med* 8:469–476.
39. Hazenberg MD, *et al.* (2000) T cell division in human immunodeficiency virus (HIV-1)-infection is mainly due to immune activation: A longitudinal analysis in patients before and during highly active anti-retroviral therapy. *Blood* 95:249–255.
40. Hamann D, *et al.* (1997) Phenotypic and functional separation of memory and effector human $CD8^+$ T cells. *J Exp Med* 186:1407–1418.
41. Baars PA, *et al.* (1995) Heterogeneity of the circulating human $CD4^+$ T cell population: Further evidence that the $CD4^+CD45RA^-CD27^-$ T cell subset contains specialized primed cells. *J Immunol* 154:17–25.
42. Previs SF, *et al.* (1996) Assay of the deuterium enrichment of water via acetylene. *J Mass Spectrom* 31:639–642.
43. Patterson BW, Zhao G, Klein S (1998) Improved accuracy and precision of gas chromatography/mass spectrometry measurements for metabolic tracers. *Metabolism* 47:706–712.
44. Henderson AR (2005) The bootstrap: A technique for data-driven statistics. Using computer-intensive analyses to explore experimental data. *Clin Chim Acta* 359:1–26.
45. Westermann J, Pabst R (1990) Lymphocyte subsets in the blood: A diagnostic window on the lymphoid system? *Immunol Today* 11:406–410.

Supporting Information

Vrisekoop *et al.* 10.1073/pnas.0709713105

SI Text

Mathematical Modeling. Because the fraction of heavy water in body water is similar to that in urine (1), we model the measured up- and down-labeling of the urine enrichment by the following differential equations for normal water, w, and heavy water, h, in the urine

$$\frac{dw}{dt} = (1-f)s - \delta w \quad \text{and} \quad \frac{dh}{dt} = fs - \delta h$$

during label intake ($t \leq \tau$), and

$$\frac{dw}{dt} = s - \delta w \quad \text{and} \quad \frac{dh}{dt} = -\delta h$$

after label intake ($t > \tau$), where f represents the fraction of ^2H_2O in the drinking water, t represents time in days, and labeling was stopped at $t = \tau = 63$ days. δ represents the turnover rate of body water per day, and s is the amount of water consumed in liters per day. These equations can be solved analytically and rewritten in terms of the fraction, $U(t)$, of ^2H_2O in the urine. The baseline urine enrichment, $U(0) = \beta$, that is attained after the boost of label by the end of day 0 determines the initial conditions, i.e., $w(0) = (1-\beta)s/\delta$ and $h(0) = \beta s/\delta$, such that:

$$U(t) = f(1 - e^{-\delta t}) + \beta e^{-\delta t} \qquad \textbf{[1a]}$$

during label intake ($t \leq \tau$), and

$$U(t) = [f(1 - e^{-\delta\tau}) + \beta e^{-\delta\tau}]e^{-\delta(t-\tau)} \qquad \textbf{[1b]}$$

after label intake ($t > \tau$).

The parameter estimates of the best fits for the urine curves are given in Table S2.

To model the label enrichment of adenosine in the DNA of cells we assume identical reaction kinetics of hydrogen and deuterium and of labeled and unlabeled adenosines. Further, we extended the model of Asquith *et al.* (2) to include the dependence on the actual enrichment of the body water [as estimated by $U(t)$]. Because the adenosine deoxyribose (dR) moiety contains seven hydrogen atoms that can be replaced by deuterium, one expects an amplification factor, $c > 1$, in the enrichment of dR in DNA relative to the body ^2H_2O enrichment. At the low levels of body ^2H_2O enrichment that one typically achieves [$U(t) < 2\%$], the likelihood of double labeling is very low (3, 4). Theoretically, the fraction of adenosine dR moieties that have exactly one enriched hydrogen atom is expected to be $c \cong \binom{7}{1}U(t)(1 - U(t))^6$. However, because of dilution by the purine nucleoside pathway, one typically measures the amplification factor c from the enrichment in dR in the DNA of cells with a rapid turnover, like granulocytes or monocytes (3, 4). Consistent amplification factors of $c = 3.5$ to $c = 4$ for body water enrichment levels of 2–3% are reported in ref. 4.

Following Asquith *et al.* (2), label enrichment of adenosine in the DNA of a population of cells was modeled by

$$\frac{dl}{dt} = pcU(t)A - dl,$$

where l is the total amount of labeled adenosine in the DNA, p is the average production rate of that population, c is the amplification factor, A is the total amount of adenosine in the DNA of that population, and d is the loss rate of cells carrying labeled adenosine. Basically, one writes that each adenosine residue replicates at rate p and will incorporate a deuterium atom with probability $cU(t)$. For naïve T cells, this replication may occur both in the periphery and the thymus. Scaling this equation by the total amount of adenosine in the DNA, i.e., defining $L = l/A$, yields

$$\frac{dL}{dt} = pcU(t) - dL \qquad \textbf{[2]}$$

throughout the labeling and delabeling period, where L represents the fraction of labeled deoxyribose residues of adenosine in DNA. The corresponding analytical solutions for the enrichment of adenosine in DNA are

$$L(t) = \frac{cpf}{\delta - d}\left[\frac{\delta}{d}(1 - e^{-dt}) - (1 - e^{-\delta t}) + \frac{\beta}{f}(e^{-dt} - e^{-\delta t})\right] \qquad \textbf{[3a]}$$

during label intake ($t \leq \tau$), and

$$L(t) = \frac{cpf}{\delta - d}\left[\frac{\delta}{d}(e^{-d(t-\tau)} - e^{-dt}) - (e^{-\delta(t-\tau)} - e^{-\delta t}) + \frac{\beta}{f}(e^{-dt} - e^{-\delta t})\right] \qquad \textbf{[3b]}$$

after label intake ($t > \tau$). Note that the amplification factor and the division rate always appear together, and that pc can therefore only be estimated as a parameter combination.

Eqs. **3a** and **3b** were fitted to each individual's granulocyte enrichment data, yielding $0.299 \leq pc \leq 0.419$ per day and death rates $0.078 < d < 0.103$ per day (see Table S3). Assuming that the granulocytes are fully turned-over, i.e., assuming that $p = d$ for the granulocytes, we estimate amplification factors of $c = 4.46$, 4.93, 5.15, 3.78 and $c = 4.03$ for the five individuals (which is indeed lower than the theoretical maximum of 7).

Next, Eqs. **3a** and **3b** were applied to calculate the average turnover rate p and the loss rate of labeled cells d in each T cell population. The parameter p in Eq. **2** represents T cell production resulting from both T cell proliferation and thymic output. Because p determines the average T cell turnover rate, pN (the average number of naive cells produced per day) provides an upperbound for the number of T cells exported from the thymus per day. To correct for the body water enrichment as measured by $U(t)$ and the amplification factor, c, of each individual person, all data were normalized by dividing by the maximum cf. Doing the same for the granulocyte data the maximum label enrichment in granulocytes was basically scaled to 100%.

Cells that divided during the first days of the labeling period will have incorporated less deuterium than those that divided later. If such cells were to die earlier than cells that divided later, the loss of label during the chase phase need not be exponential because poorly labeled cells would die earlier. However, because we are assuming an exponential distribution of expected life spans in these models, cells are assumed to have death rates that are independent of their age.

1. Ackermans MT, *et al.* (2001) *J Clin Endocrinol Metab* 86:2220–2226.
2. Asquith B, Debacq C, Macallan DC, Willems L, Bangham CR (2002) *Trends Immunol* 23:596–601.
3. Hellerstein MK, Neese RA (1999) *Am J Physiol* 276:E1146–E1170.
4. Neese RA, *et al.* (2002) *Proc Natl Acad Sci USA* 99:15345–15350.

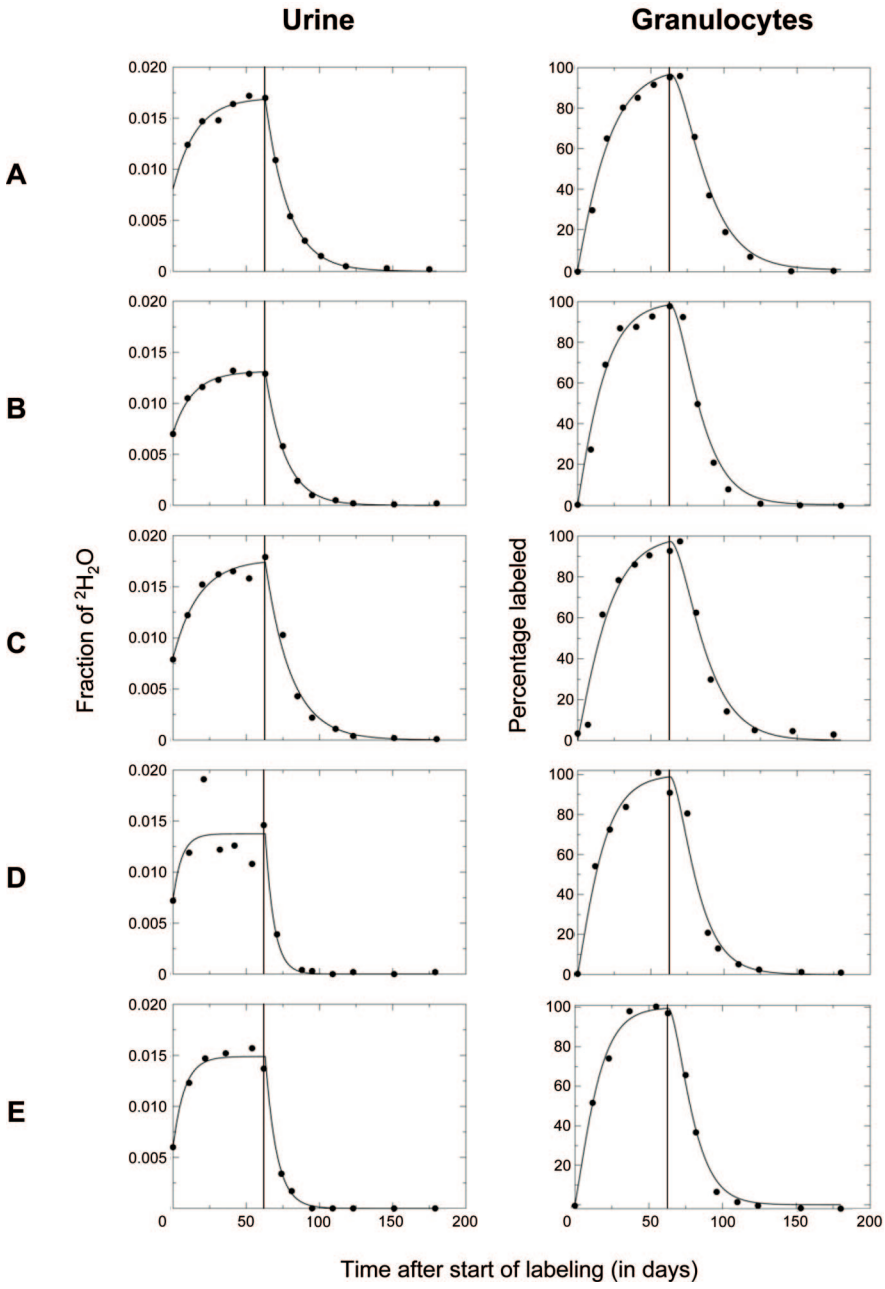

Fig. S1. Best fits of the fraction of ^2H_2O in urine and the percentage of labeled deoxyribose residues of adenosine in granulocytes after scaling by the maximum enrichment level *cf* of the granulocyte population (see *SI Text*). In the graph, the end of the labeling period is marked by a vertical line.

Table S1. Characteristics of healthy volunteers

Characteristic	Individual				
	A	B	C	D	E
Age at start of the protocol	24	22	25	20	22
$CD4^+$ count per μl blood	890 (810–1040)	690 (663–808)	830 (780–990)	1300 (1080–1730)	1320 (1130–1500)
$CD8^+$ count per μl blood	470 (420–550)	355 (320–413)	500 (460–590)	440 (410–530)	820 (660–910)
Naïve $CD4^+$, %	60 (54–66)	68 (65–71)	37 (34–41)	69 (67–73)	68 (63–71)
Memory $CD4^+$, %	40 (34–45)	32 (29–34)	54 (48–56)	31 (27–33)	31 (28–36)
Naïve $CD8^+$, %	54 (50–58)	68 (63–70)	37 (31–41)	65 (62–71)	59 (52–62)
Memory $CD8^+$, %	35 (29–40)	17 (14–18)	18 (15–21)	12 (11–14)	20 (19–21)
$Ki67^+$ within $CD4^+$, %	2.75 (2.33–3.19)	1.86 (1.47–2.25)	2.13 (1.82–2.30)	1.36 (0.59–2.18)	1.61 (1.37–2.12)
$Ki67^+$ within naïve $CD4^+$, %	0.76 (0.39–1.05)	0.91 (0.65–1.24)	0.77 (0.59–0.99)	0.29 (0.21–1.40)	0.43 (0.33–0.73)
$Ki67^+$ within memory $CD4^+$, %	5.00 (4.29–5.02)	3.42 (2.93–4.45)	3.18 (2.87–3.52)	1.82 (1.55–2.50)	3.84 (3.05–4.24)
$Ki67^+$ within $CD8^+$, %	1.65 (1.45–1.88)	1.46 (1.26–1.92)	2.29 (1.68–2.78)	1.26 (0.85–1.72)	1.34 (1.14–1.81)
$Ki67^+$ within naïve $CD8^+$, %	0.94 (0.57–1.12)	0.73 (0.57–1.13)	0.97 (0.63–1.21)	0.47 (0.22–0.68)	0.50 (0.42–0.65)
$Ki67^+$ within memory $CD8^+$, %	1.87 (1.61–2.05)	2.35 (1.98–2.97)	NA	1.51 (1.22–2.51)	3.54 (2.46–4.01)

Depicted are median values and interquartile ranges over follow-up.

Table S2. Parameter estimates of the urine enrichment curves, where f represents the fraction of ^2H_2O in the drinking water, δ is the turnover rate of body water per day, and β represents the baseline urine enrichment attained after the boost of label by the end of day 0

Individual	f	δ	β
A	0.0170	0.064	0.0080
B	0.0129	0.088	0.0070
C	0.0173	0.075	0.0082
D	0.0138	0.128	0.0074
E	0.0150	0.119	0.0059

Table S3. Parameter estimates of the granulocyte enrichment curves (before scaling), where *d* represents the loss rate of labeled granulocytes, *p* is the average production rate of granulocytes, and *c* the amplification factor

Individual	*pc*	*d*
A	0.384	0.086
B	0.419	0.085
C	0.402	0.078
D	0.299	0.079
E	0.415	0.103

Other Supporting Information Files

Dataset S1